

Non-linear dynamic analysis of an adobe module

Nicola Tarque Ruíz

Division of Civil Engineering, Pontificia Universidad Católica del Perú
Av. Universitaria 1801, San Miguel, Lima 32, Peru
Tel.: +51-1-6262000 IP 4610; Fax: +51-1-6262813
E-mail: sntarque@pucp.edu.pe

Guido Camata

Università degli Studi 'G. D'Annunzio' Chieti-Pescara
Viale Pindaro 42, 65127 Pescara, Italy
Tel.: +39-085-4537276; Fax +39-085-4537255
E-mail: guido.camata@colorado.edu

Enrico Spacone

Università degli Studi 'G. D'Annunzio' Chieti-Pescara
Viale Pindaro 42, 65127 Pescara, Italy
Tel.: +39-085-4537276; Fax +39-085-4537255
E-mail: espacone@unich.it

Humberto Varum

Division of Civil Engineering, University of Aveiro
Campus Universitário de Santiago, 3810-193 Aveiro, Portugal
Tel.: +351-234-370049; Fax: +351-234-370094
E-mail: hvarum@ua.pt

Marcial Blondet

Division of Civil Engineering, Pontificia Universidad Católica del Perú
Av. Universitaria 1801, San Miguel, Lima 32, Peru
Tel.: +51-1-6262000 IP 4610; Fax: +51-1-6262813
E-mail: mblondet@pucp.pe

Theme 6: Research in Materials and Technology for Conservation and Contemporary Architecture.

Key words: adobe building, non-linear dynamic analysis, continuum model, damaged plasticity based model

Abstract

In a preliminary numerical analysis of an adobe wall carried out by the authors, the material properties in compression and tension of the adobe masonry were calibrated to represent its seismic in-plane behaviour. Now, the preliminary work is extended to the analysis of a full-scaled adobe module, dynamically tested at the Catholic University of Peru in 2005, considering the in-plane and out-of-plane actions through a finite element model.

The adobe material is considered brittle. The inelastic part of the tension is represented by a softening curve and the compression is characterized by a hardening/softening part. In this work a finite element model, using a continuous approach, is created in the program Abaqus/Explicit for simulating an adobe module. The damage evolution in the numerical simulation represents fairly well the crack pattern observed in the adobe module, for in-plane and out-of-plane actions. It is concluded, that the calibrated material properties and the explicit solution scheme are good tools for analyzing the seismic capacity of other unreinforced adobe structures: historical and vernacular.

1. INTRODUCTION

Adobe and adobe constructions have some attractive characteristics, such as low cost, local availability, self/owner-made or no need for skilled labour (hence the name “non-engineered constructions”), good thermal insulation and acoustic properties (Memari & Kauffman 2005). However, adobe constructions don't perform well under seismic excitation and for this reason they are vulnerable in earthquake-prone regions. Thus, in order to improve their dynamic performance and to reduce the seismic vulnerability, it is important to study their seismic behaviour through experimental and numerical analyses. The biggest challenge to model properly the adobe constructions is the correct characterization of the material properties (especially in the inelastic range) and the correct geometric description of the structural components. Some inelastic material properties cannot be found experimentally; therefore, it is important to calibrate them numerically in order to describe properly the seismic behaviour of adobe constructions.

This paper presents an attempt to capture the dynamic response and failure analysis of an adobe module using a nonlinear finite element model. For this, a continuum model called Concrete Damage Plasticity, which is implemented in the finite element program Abaqus/Explicit, is used to represent the adobe masonry as a homogeneous and isotropic material.

2. ANALYSIS METHOD

2.1 Finite element modelling

The masonry material can be numerically modelled following a discrete or continuum mechanic approach (e.g. Lotfi and Shing 1994; Lourenço 1996; Ngo and Scordelis 1967; Roca et al. 2010). The first assumes that the damage is concentrated at specific zones to simulate the block-to-block and block-to-mortar interaction (Roca *et al.* 2010). Generally the inelasticity behaviour is concentrated at the mortar joints to represent tension, shear and compression failure of the masonry. In this case the unit blocks (bricks) and the joint mortar are modelled using different finite elements. If the failure mechanism is known and the crack path can be identified, the discrete model accurately represents the actual cracking observed in the tests. The second approach, continuum model, predicts cracking and damage distributed all over the continuum, where a description of the interaction between bricks and mortar is not necessary since there is not physical difference between blocks and joint mortar. The crack propagation is mainly controlled by the shape of the tensile-softening diagram and the material fracture energy (Cruz *et al.* 2004).

The failure assessment of concrete and masonry structures is mainly dependent on the material constitutive laws (Feenstra & de Borst 1992; Feenstra & Rots 2001). Similarly to concrete, adobe masonry behaves well under compression, but can only resist low tensile stresses with a quite brittle post-peak tensile behaviour. Since the adobe bricks and the mortar are composed of mud, both can be assumed as a homogeneous and isotropic material. The adobe module examined in this paper is composed of adobe bricks, mud mortar, concrete foundation and a timber roof. The adobe bricks and the mud mortar are supposed to be a unique material and modelled with the concrete damaged plasticity model (continuum approach).

2.2 Continuum approach: the concrete damaged plasticity model

The concrete damaged plasticity model implemented in Abaqus/Explicit is developed for quasi-brittle materials subjected to cyclic loads and uses concepts of isotropic damaged elasticity in combination with isotropic tensile and compressive plasticity to represent the inelastic behaviour of the material. This model is based on the work developed by Lubliner *et al.* (1989) and by Lee and Fenves (1998), where the two main failure mechanisms are the tensile cracking and the compressive crushing of the material. This model assumes that failure of the material can be effectively modelled using its uniaxial tension, uniaxial compression and plasticity characteristics (Figure 1). In this work, an exponential and a

parabolic curve has been selected for modelling the tension and the compression behaviour of the adobe material in the inelastic range, respectively. The function parameters and the evaluation of the fracture energies are defined by Lourenço (1996) based on masonry tests.

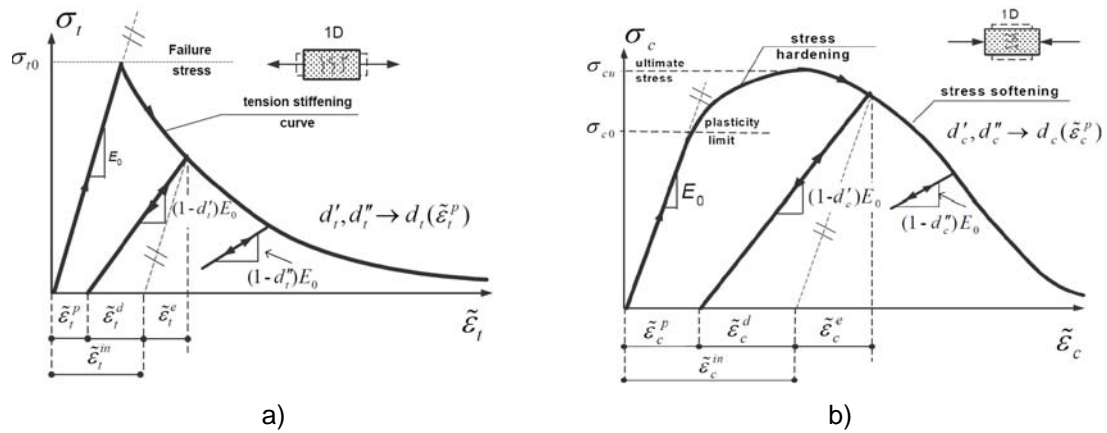


Figure 1. Model response under compression and tension loads implemented in Abaqus for the Concrete damaged plasticity model, a) Tension behaviour, b) Compression behaviour (modified from Wawrzynek and Cincio 2005).

The total strain is decomposed additively into the elastic and plastic strain, $\varepsilon = \varepsilon_e + \varepsilon_p$. Cracking in the plasticity-based model is represented by the damage factors, d_t and d_c , that reduce the elasticity module in tension and compression under reversal loads (Figure 1). When the material goes from tension to compression or viceversa, the parameters ω_c and ω_t controls the recovery of the compressive and tensile stiffness, respectively. The plastic deformation is defined as an irreversible process that dissipates energy as it proceeds (Boger 2006).

3. EXPERIMENTAL TEST AT THE CATHOLIC UNIVERSITY OF PERU

Blondet *et al.* (2006) carried out a dynamic test on an adobe module to analyze the seismic response and the damage pattern evolution on the adobe masonry. The unidirectional dynamic test was performed on an adobe module built over a reinforced concrete ring beam to facilitate the anchor of the specimen to the unidirectional shake table. The total weight (module + foundation) was around 135 kN. The weight of the concrete beam was 30 kN. The adobe bricks and the mud mortar used for the construction of the module had a soil/coarse sand/straw proportion of 5/1/1 and 3/1/1; respectively. The module consisted of four walls 3.21 m long, identified as right, left, front and rear wall. The wall thickness of the right wall was 0.28 m because it had mud stucco, while the other walls had 0.25 m. wall thickness (Figure 2).

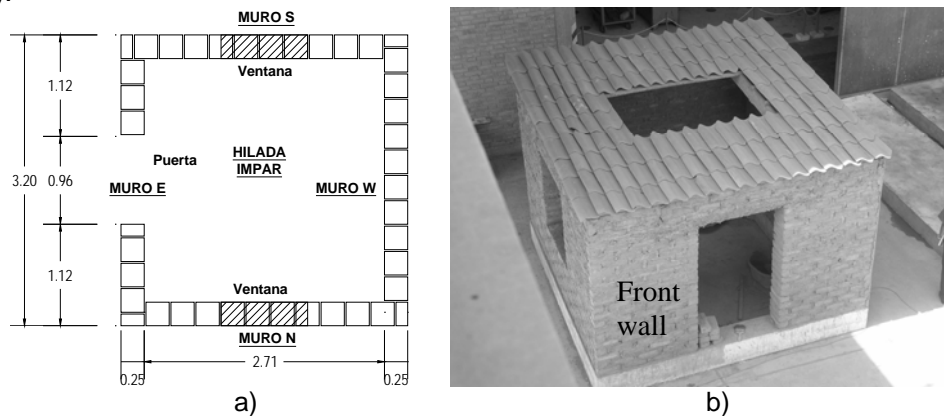


Figure 2. Adobe module tested at the PUCP, a) dimensions on a plan view, b) 3D view of the adobe module.

The longitudinal walls (parallel to the direction of the displacement signal) included a central window opening. The front wall had a door opening and the rear wall did not have any openings. All the adobe walls were built considering normal stretcher bond. The roof consisted of wooden joists covered with cement tiles, the wooden were attached to the walls with steel nails. The idea of the module was to represent a part of a typical vernacular Peruvian adobe building within the limitations of the 4.0x4.0 m shake table, which allows a maximum specimen weight of 160 kN.

The adobe module was unidirectional subjected to three levels of displacement signals, which were scaled to have maximum displacements of 30, 80 and 120 mm at the base, the input displacement signals are related to PGA of 0.3, 0.8 and 1.2g, respectively. For convenience, the displacement input related to Phase 2 is showed in Figure 3. These earthquake levels (phases) intend to represent the effects of a frequently, moderate and severe earthquake on the adobe buildings. The input signals were scaled from an acceleration record of one Peruvian earthquake occurred in 1970.

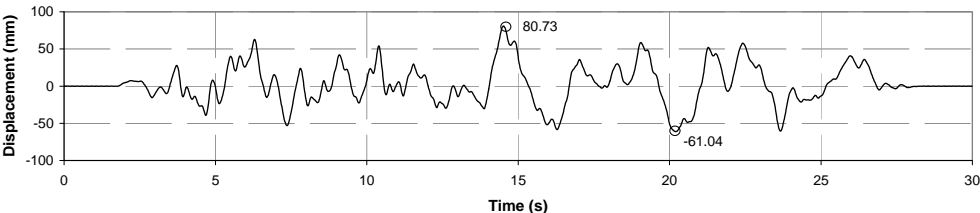


Figure 3. Displacement input used in Phase 2 and scaled to have maximum amplitude of 80 mm.

Ten accelerometers and 8 LVDT were left in the model distributed in all the walls, and 1 accelerometer and 1 LVDT were left at the shaking table (Figure 4). The module was tested after more or less two weeks from the end of the construction.

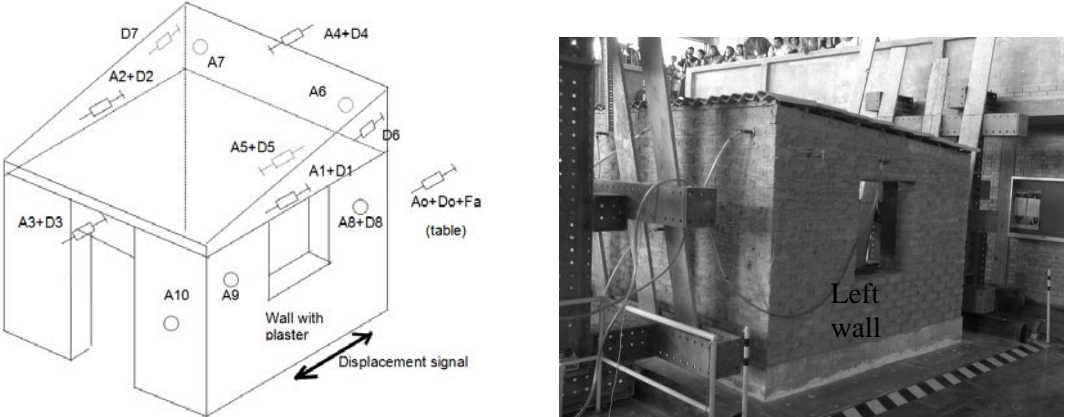


Figure 4. Disposition of the accelerometers and LVDTs on the adobe module.

3.1 Damage description

The displacement signals were applied parallel to the two walls with window (identified as Right and Left Wall). At the end of the Phase 1 and during the Phase 2 typical vertical cracks appeared at the wall intersections causing the separation of the walls; then, x-shape cracks appeared at the longitudinal walls, and cracks due to horizontal and vertical bending appeared at the transverse walls. The anchorage of the steel nails that connected the wooden beams with the walls was lost during the movement, and as a result the roof was supported by the walls just by its own weight and by friction. Major damage was observed during the second phase and a total collapse was observed during the third phase. The Left Wall, which had stucco, was stiffer than the other walls. The difference in stiffness from the two parallel walls triggered torsional effects in the structure during the second and third phases. The displacement response of each wall is showed later in section 4.2.

The Rear Wall, which was itself broken more or less into 3 big blocks (typical of walls supporting just by three sides), had a rocking behaviour due to out-of-plane actions. During the third phase, which maximum displacement of 130 *mm* at the base, the perpendicular walls fell down at the beginning of the input signal while the parallel walls were completely cracked. Since the roof was supported by the lateral walls, it did not collapse. In this work the second phase is reproduced with the numerical model.

The vertical cracks at the wall intersections vary in thickness according to the amplitude of the signal. From the displacement histories reported by the LVDT during the phase 2, it is seen that all the walls have a maximum relative displacement right after 10 s of signal (see section 4.2), where the vertical cracks seem to reach its maximum value. After this, the two walls parallel to the movement move as a rigid body, while the two perpendicular walls move back and forth within a rocking behaviour. The formation of vertical cracks made possible the separation of walls, allowing them to move independently. Besides, it can be seen from the displacement time history that after the walls separate from each other, the stiffer wall was the Right Wall.

4. NUMERICAL STUDIES

4.1 Description of the model and material properties

A finite element model is created in Abaqus to simulate the non-linear dynamic response during the phase 2 of the adobe module presented before (Figure 5). The foundation (concrete ring beam), the adobe walls, the lintels and two internal wooden beams are represented by plane-stress shell elements. The other wooden beams (placed above the walls with windows) and the joints are modelled with beam elements. The foundation is fully fixed at the base during the application of gravity loads; after this, just one displacement DOF in the direction of the movement is released in order to apply the acceleration at the base. The perimetral wooden beams were reduced in length to avoid a rigid connection between them; in this case, the walls can develop vertical cracks at the intersections without any additional restriction due to the ring beam (Figure 5 right). This model does not simulate the real interaction between the wooden beams and the adobe walls, since there is not enough information about the resistance of the steel nails inside the adobe bricks. The internal wooden beams were modelled using shell elements to distribute the stresses among more contact points between the beams and the perpendicular adobe walls, this avoid stress concentration.

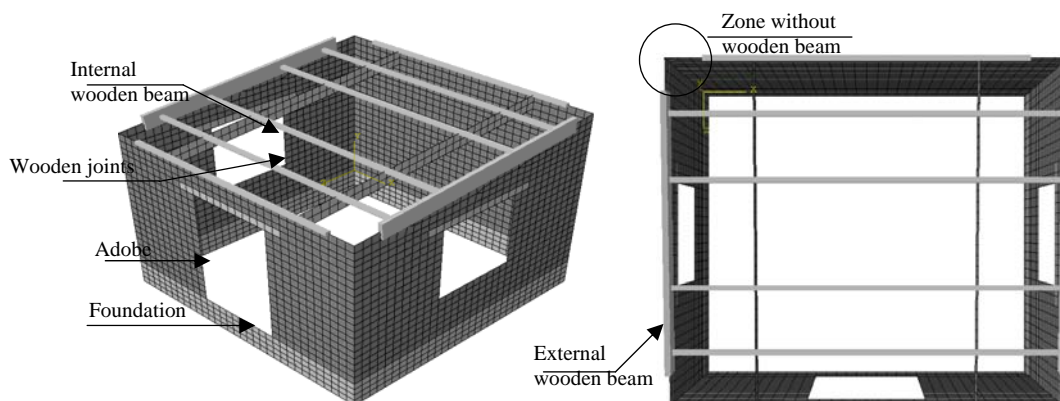


Figure 5. Finite element model of the adobe module built in Abaqus/Explicit.

The model consists of 3406 nodes, 232 linear line elements B31, 3038 quadrilateral 4-nodes shell elements S4 (full integration), and 6 triangular 3-nodes shell elements S3 (full integration). All the walls have 5 Gauss integration points through the thickness. The thickness of the right wall is 280 *mm* and the thickness of the other walls is 250 *mm*. The mesh size is, in majority, kept as 100 x 100 *mm*, obtaining in this way a characteristic length

$h = 141.4 \text{ mm}$. The total mass of the model is $14.21 \text{ N}\cdot\text{s}^2/\text{mm}$ considering the concrete and wooden elements.

The concrete and the wooden materials are modelled elastically, whereas the adobe walls are modelled with the concrete damaged plasticity model. The material properties for adobe are the ones calibrated by Tarque (2011) and specified in Table 1, Table 2 and Figure 6. To represent the degradation of the elastic stiffness due to reversal loads, the following pairs of tensile damage factors (d_t) and tensile plastic displacements are assumed considering a characteristic length $h = 141.4 \text{ mm}$: (0.00; 0.00), (0.85; 0.125), (0.90; 0.25), (0.95; 0.50). The stiffness recovery in compression, w_c , is 0.5 and in tension, w_t , is 0.0. Besides, the concrete damaged plasticity model requires 4 more parameters for a complete description of the yield surface: the dilatancy angle, the eccentricity, the relation between the initial equibiaxial compressive yield stress to initial uniaxial compressive yield stress and a parameter that defines the shape of the yield surface in the deviatoric plane, these values were 1, 0.1, 1.16 and $2/3$, respectively.

Table 1. Elastic material properties of the adobe blocks, concrete and timber materials.

| Concrete | | | Timber | | |
|-------------------|-------|------------------------------------|-------------------|-------|------------------------------------|
| $E \text{ (MPa)}$ | ν | $\gamma_m \text{ (N/mm}^2\text{)}$ | $E \text{ (MPa)}$ | ν | $\gamma_m \text{ (N/mm}^2\text{)}$ |
| 22000 | 0.25 | 2.4e-05 | 10000 | 0.15 | 6.87e-06 |

Table 2. Material properties for the adobe masonry within the concrete damaged plasticity model.

| Elastic | | | | Tension | | Compression | | |
|-----------------------------|-------|------------------------------------|------------------|-------------------------------|------------------------|-------------------------------|------------------------|---------------------------------|
| $E \text{ (N/mm}^2\text{)}$ | ν | $\gamma_m \text{ (N/mm}^2\text{)}$ | $h \text{ (mm)}$ | $f_t \text{ (N/mm}^2\text{)}$ | $G_f^t \text{ (N/mm)}$ | $f_c \text{ (N/mm}^2\text{)}$ | $G_f^c \text{ (N/mm)}$ | $\varepsilon_p \text{ (mm/mm)}$ |
| 200 | 0.2 | 2e-05 | 141.4 | 0.04 | 0.01 | 0.45 | 0.155 | 0.002 |

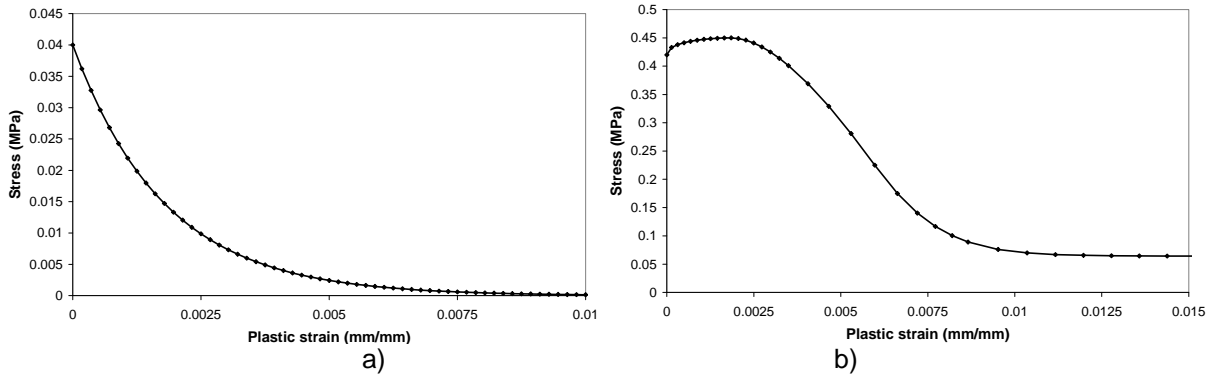


Figure 6. Constitutive laws for the adobe material, a) tension, b) compression.

4.2 Numerical results

The gravity load is applied using an implicit strategy in Abaqus/Standard. Afterwards, the results are loaded into Abaqus/Explicit and the horizontal acceleration is applied at the base. The numerical model reproduces just the Phase 2 of the experimental test. Abaqus/Explicit makes use of the central difference integration rule for integration of the equation of motions, which is more convenient when dealing with dynamic problems. The global stable time increment computed by Abaqus was $4.5018 \text{ e-}06 \text{ s}$. Here it is assumed that the energy dissipation in the model is completely given by the hysteretic behaviour of the adobe material.

The crack pattern observed in the numerical results depicts fairly well the one observed in the experimental test: diagonal cracks appears at the Right and Left walls, which are parallel to the movement, and cracks due to vertical and horizontal bending appear at the

perpendicular walls: Front and Rear walls. Figure 7 shows the tensile plastic strains of the numerical model at the end of the 30s acceleration signal. From the comparison of the two walls parallel to the movement, it is seen that the right wall is stiffer than the left wall due to the presence of the mud plaster. The no connection of the wooden beams at the corners allows the development of vertical cracks at the wall intersections, so a rocking behaviour at the walls perpendicular to the movement can be simulated.

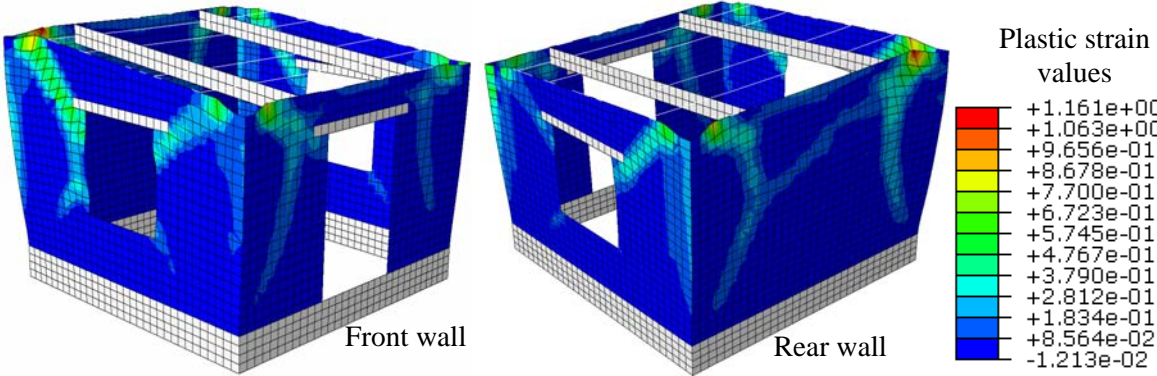


Figure 7. Tensile plastic strain of the numerical model built with concrete damaged plasticity.

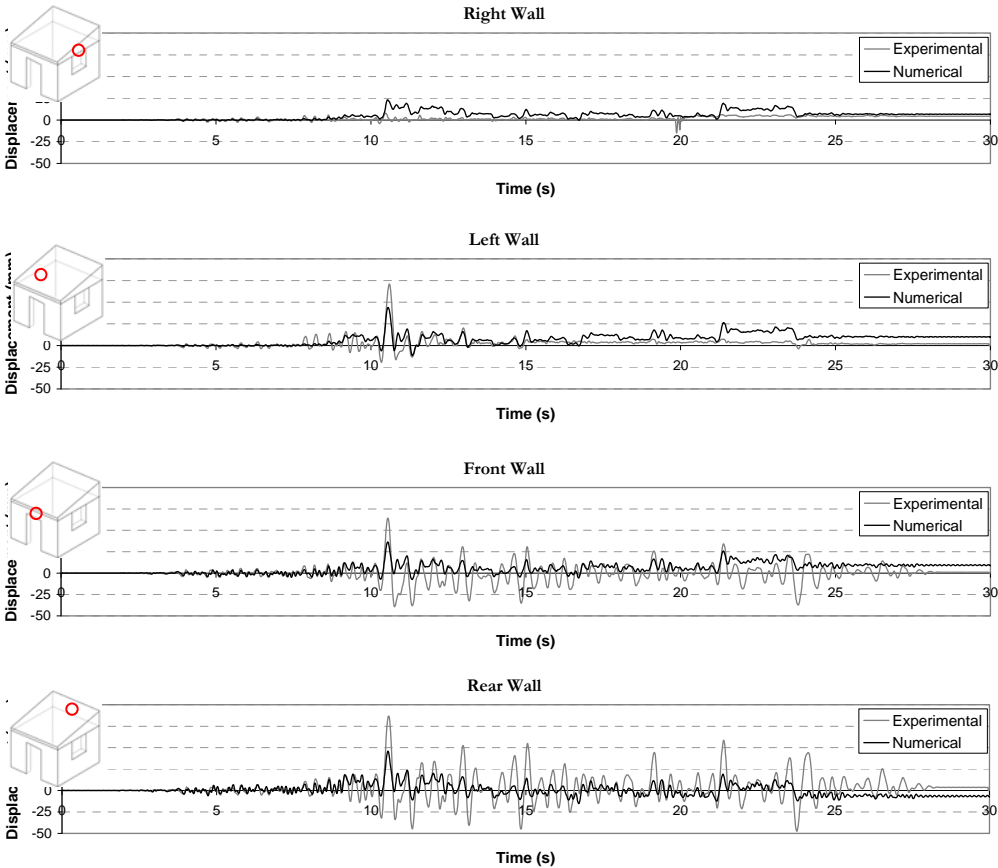


Figure 8. Experimental vs numerical displacement history of the adobe walls measured at the top.

Figure 8 shows that the maximum relative displacement is around 10 s. Afterwards, the walls oscillate from a new equilibrium position indicating a residual inelastic displacement. The numerical rocking behaviour of the two walls perpendicular to the movement, in particular the out of plane displacement, differ from the experimental behavior because this numerical model does not allow the elimination of the shell elements that reach the maximum tensile

plastic strain, so it is not possible to obtain a completely independent behaviour between perpendicular walls. However, the model captures the failure and it is useful to understand the seismic behaviour of the adobe structure in terms of failure mechanisms. Figure 8 shows that the numerical relative displacement of the front and rear walls depends on the relative displacements of the right and left walls, which are parallel to the movement.

5. CONCLUSIONS

This paper deals with the numerical non-linear dynamic analysis of an adobe module, previously tested at the Catholic University of Peru, following a continuum approach in Abaqus/Implicit and Abaqus/Explicit. The used constitutive model was the concrete damaged plasticity model, which assumes the adobe as an isotropic material. Besides, the adobe masonry can be considered as a homogeneous material represented by its tensile and compressive constitutive laws. The material properties (elastic and inelastic) were calibrated in a previous work by the authors (Tarque 2011) based on an experimental in-plane cyclic test on an adobe wall.

The numerical model is subjected to an acceleration record at the base related to the Phase 2 of the experimental test, which had a maximum base displacement of 80 mm. The numerical results represented fairly well the real crack pattern, failure mechanisms and displacement response, which validates the procedure following here for modelling the adobe module. To simulate the poor connection seen between the wooden beams of the roof and the adobe walls, the wooden beam elements were reduced in length to avoid a physical connection at the wall corners (see Figure 5).

The calibrated material properties proposed by the authors and the procedure for modelling adobe structures seen here are good enough for representing the non-linear dynamic response of adobe buildings under seismic excitations.

REFERENCES

- Blondet, M. et al., 2006. Experimental Study of Synthetic Mesh Reinforcement of Historical Adobe Buildings. In P. B. Lourenço et al., eds. *Proceedings of Structural Analysis of Historical Constructions*. New Delhi, India, pp. 1-8.
- Boger, R., 2006. *Non-monotonic strain hardening and its constitutive representation*. Ph.D. Thesis. Ohio, United States: The Ohio State University.
- Feenstra, P.H. & de Borst, R., 1992. The use of various crack models in F.E. analysis of reinforced concrete panels. In Z. P. Bažant, ed. *Proceedings of First International Conference on Fracture Mechanics of Concrete Structures: FraMCoS1*. Breckenridge, Colorado, USA: Taylor and Francis. Available at: http://books.google.com/books?id=IOOxo8bRz1sC&pg=PA379&lpg=PA379&dq=total+strain+smear+crack+model&source=bl&ots=Rq7TDXv5uL&sig=3di0rIkbtRApcOb2pRAKmWMPQs&hl=en&ei=Qi32TYuHH4_QsgbkwondBg&sa=X&oi=book_result&ct=result&resnum=5&ved=0CDQQ6AEwBA#v=onepage&q=total strain smear crack model&f=false.
- Feenstra, P.H. & Rots, J.G., 2001. Comparison of Concrete Models for Cyclic Loading. In P. B. Shing & T.-aki Tanabe, eds. *Modelling of Inelastic Behaviour of RC Structures under Seismic Loads*. USA: American Society of Civil Engineers, pp. 38-55. Available at: <http://books.google.com/books?id=NIG-PtPuyJsC&pg=PA39&lpg=PA39&dq=concrete+damaged+plasticity,+decomposed+strai>

n+model&source=bl&ots=KXt9UFRCHQ&sig=F1pJeI09__gINR3rZrGN9vKDsYA&hl=en&ei=7z5ITdidB4rsOe7L1c4E&sa=X&oi=book_result&ct=result&resnum=1&ved=0CBoQ6AEwAA#v=onepage&q=concrete damaged plasticity%2C decomposed strain model&f=false.

- Lee, J. & Fenves, G.L., 1998. Plastic-Damage Model for Cyclic Loading of Concrete Structures. *Journal of Engineering Mechanics*, 124(8), pp.892-900. Available at: <http://link.aip.org/link/JENMDT/v124/i8/p892/s1&Agg=doi> [Accessed May 19, 2011].
- Lotfi, H.R. & Shing, P.B., 1994. Interface Model Applied to fracture of masonry Structures. *ASCE*, 120(1), pp.63-80.
- Lourenço, P.B., 1996. *Computational strategies for masonry structures*. Ph.D. Thesis. Delft, The Netherlands: Delft University.
- Lubliner, J. et al., 1989. A plastic-damage model for concrete. *International Journal of Solids and Structures*, 25(3), pp.299-326. Available at: <http://linkinghub.elsevier.com/retrieve/pii/0020768389900504>.
- Memari, A.M. & Kauffman, A., 2005. Review of Existing Seismic Retrofit Methodologies for Adobe Dwellings and Introduction of a New Concept. In *Proceedings of SismoAdobe2005*. Lima, Peru: Pontificia Universidad Católica del Perú, p. 15.
- Ngo, D. & Scordelis, A.C., 1967. Finite Element Analysis of Reinforced Concrete Beams. *American Concrete Institute*, 64(3), pp.152-163.
- Page, A.W., 1978. Finite element model for masonry. *Journal of Structural Engineering*, 104(8), pp.1267-1285.
- Pelà, L., 2008. *Continuum damage model for nonlinear analysis of masonry structures*. Ph.D. Thesis. Ferrara, Italy: Università degli Studi di Ferrara.
- Roca, P. et al., 2010. Structural Analysis of Masonry Historical Constructions. Classical and Advanced Approaches. *Archives of Computational Methods in Engineering*, 17(3), pp.299-325. Available at: <http://www.springerlink.com/index/10.1007/s11831-010-9046-1> [Accessed March 7, 2011].
- Rots, J.G., 1991. Numerical simulation of cracking in structural masonry. *Heron*, 36(2), pp.49-63.
- Tarque Ruíz, N., 2011. *Numerical modelling of the seismic behaviour of adobe buildings*. Ph.D. Thesis. Pavia, Italy: ROSE School, Istituto di Studi Superiori di Pavia IUSS.
- Wawrzynek, A. & Cincio, A., 2005. Plastic-damage macro-model for non-linear masonry structures subjected to cyclic or dynamic loads. In *Proceedings of Conf. Analytical Models and New Concepts in Concrete and Masonry Structures, AMCM'2005*. Gliwice, Poland. Available at: <http://kateko.rb.polsl.pl/katedra/sylwetki/publikacje/awaw/AMCM-A50f.pdf>.

Curriculum:

Nicola Tarque is a Lecturer at the Catholic University of Peru and PhD candidate at ROSE School – Istituto Universitario di Studi Superiori di Pavia, Italy. His main research topics include masonry constructions and seismic risk assessment.

Guido Camata is an Assistant Professor of Structural Engineering at the University of Chieti-Pescara. He worked at ISIS Canada (Intelligent Sensing for Innovative Structures) in Winnipeg, Canada, and after at the University of Colorado at Boulder. His research experience includes both experimental and numerical work.

Enrico Spacone, a professor of Structural Engineering, is Chair of the department of Engineering at the University of Chieti-Pescara. His research focuses on modelling and analysis of structures under seismic loads.

Humberto Varum, Associate Professor at the Civil Engineering Department, University of Aveiro, Portugal, member of the National Committee of ICOMOS. His main research interests include earth construction characterization and seismic strengthening.

Marcial Blondet is Professor of Civil Engineering at the Catholic University of Peru. He obtained Masters and PhD degrees in Engineering at the University of California, Berkeley. Professor Blondet is a specialist in earthquake engineering and structural dynamics, and has ample experience on the experimental study of the seismic behaviour of structures. His main research interests are the use of energy dissipation and base isolation systems for the seismic protection of buildings, the development of low-cost solutions to mitigate the seismic risk of informal earthen and masonry dwellings, and the conservation of earthen historical monuments in seismic areas.